RECENT TESTS OF QCD WITH THE ATLAS DETECTOR*

Giuseppe Callea

on behalf of the ATLAS Collaboration

Università della Calabria and INFN Cosenza, Italy

(Received May 28, 2019)

A summary of the recent ATLAS results at the LHC in Quantum Chromodynamics is given, covering a number of areas that reflect the work of the collaboration on the Bose–Einstein correlations in multi-particle events, the inclusive jet production, the measurements of jet substructure quantities in di-jet events, and the photon–photon scattering exclusive processes.

DOI:10.5506/APhysPolBSupp.13.9

1. Introduction

The ATLAS Collaboration [1] at the LHC has a large program to study various aspects of Quantum Chromodynamics. In this contribution, the latest results on the Bose–Einstein correlations measured with the ATLAS detector are reviewed, along with an analysis of the momentum difference between charged hadrons. At higher energy scales, a measurement of the first jet substructure quantity at a hadron collider, for which accurate next-to-next-to-leading-logarithm (NNLL) predictions are available, is presented. The soft-drop mass is measured in di-jet events with the ATLAS detector at 13 TeV and compared to Monte Carlo simulations. Perturbative QCD at highest energies can be precisely tested with the measurement of particle jet production of which we present the latest results based on data collected at 8 TeV and 13 TeV. Exclusive processes can be distinguished in ATLAS exploiting the large rapidity gap in the central region and the absence of charged particles reconstructed in the inner detector. This strategy has been exploited to study the exclusive production of di-lepton pairs in the data taken at 7 TeV, exclusive di-muon production at 13 TeV, and the exclusive production of W pairs in the 8 TeV data.

* Presented at "Excited QCD 2018", Kopaonik, Serbia, March 11–15, 2018.

2. Study of ordered hadron chains

In MC simulations based on the Lund string model, such as PYTHIA, the colour string is postulated as a linear object that splits along its length. More complex types of colour connection are in principle possible, and ATLAS has studied a proposal based on a helical string structure, using the 7 TeV dataset [2]. Minimum-bias events are selected and triplets of charged tracks are studied by finding the like-sign track pair with the smallest value of $Q^2 = -(p_i - p_j)^2$, and then identifying the third opposite-sign track which minimises the overall triplet mass. A Dalitz plot is then constructed in terms of the kinetic energy of the hadrons.

Figure 1 shows the Dalitz plot that is obtained using events generated by PYTHIA (left), where a featureless plateau is seen. On the other hand, the Dalitz plot obtained from the data (right), shows indications of narrow structures at low X and high Y, incompatible with the MC models that have been studied. Figure 1 includes some indications of the type of structure that the helical string model predicts, which are in qualitative agreement with the data and give support for further investigation of this type of model.

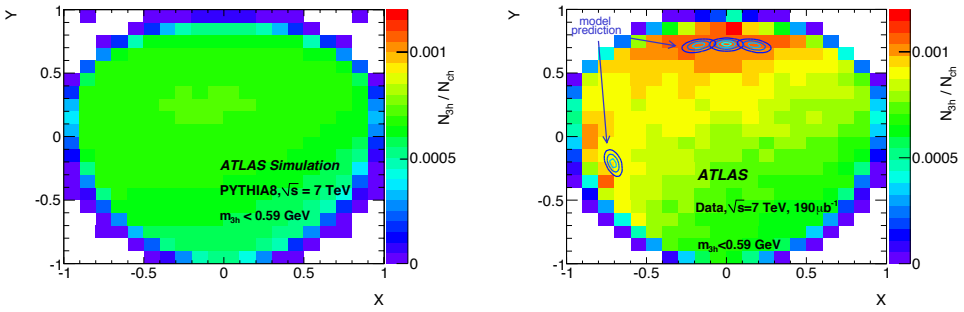


Fig. 1. Left: Dalitz plot of variables X and Y obtained using PYTHIA. Right: Dalitz plot from data, on which are superposed model predictions involving $\pi^+\pi^-\pi^0\pi^+$ combinations with unobserved π^0, at $X \approx -0.7$, and triplets of charged pions with and without a further unobserved particle, at $Y \approx 0.7$ [2].

3. Jet production

3.1. Soft drop mass measurement at 13 TeV

The first measurement of jet substructure quantity at a hadron collider, for which accurate NNLL predictions are available, has been performed with the soft-drop algorithm, using the 32.9 fb^{-1} ATLAS dataset at 13 TeV [3]. This algorithm is a jet grooming procedure that reclusters the anti-k_{T} jet's constituents with the Cambridge–Aachen algorithm, with the goal of re-

moving soft and wide angle radiation from a jet. The clustering tree is then traversed from the last branch to the earliest, applying the following criterion to the proto-jets:

$$\frac{\min(p_{\mathrm{T},1}, p_{\mathrm{T},2})}{p_{\mathrm{T},1} + p_{\mathrm{T},2}} > z_{\mathrm{cut}} \times \left(\frac{\Delta R_{12}}{R}\right)^{\beta}, \tag{1}$$

where z_{cut} and β are the algorithm parameters, which set the scale of the energy removed by the algorithm and tune the sensitivity of the algorithm to wide-angle radiation respectively. ΔR_{12} is the distance between the jets. If Eq. (1) is not satisfied, the branch with smaller p_{T} is removed and the procedure is iterated on the remaining branches, until the condition is satisfied. The mass of the resulting jet is referred to as the soft-drop jet mass, $m^{\mathrm{soft-drop}}$. In this measurement, the distribution of $\log_{10}(\rho^2)$, with $\rho = m^{\mathrm{soft-drop}}/p_{\mathrm{T}}^{\mathrm{ungroomed}}$ is studied. In Fig. 2, the unfolded data are compared to the NLO+NNLL and LO+NNLL predictions as well as to the simulations of PYTHIA, Sherpa and Herwig. The measured and predicted shapes are in good agreement in the resummation region, *i.e.* $-3.7 < \log_{10}(\rho^2) < -1.7$, where the calculations are well-defined perturbatively. The NLO+NNLL calculation contains non-perturbative corrections and continues to agree well for more negative values of $\log_{10}(\rho^2)$.

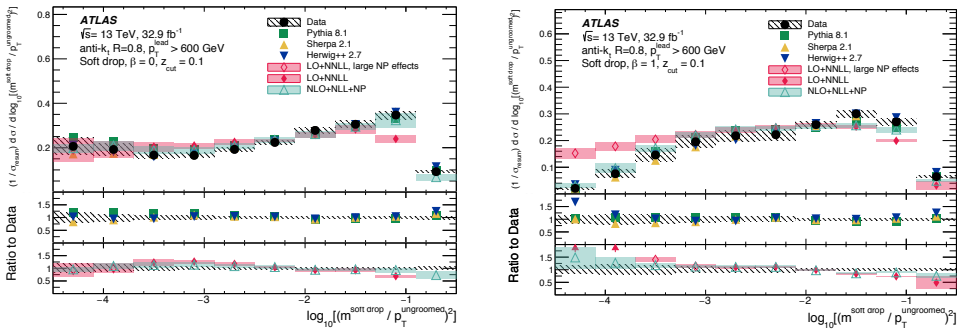


Fig. 2. The unfolded $\log_{10}(\rho^2)$ distribution after applying the soft-drop algorithm for $\beta = 0$ (left) and $\beta = 1$ (right), in data compared to PYTHIA, Sherpa and Herwig++ at particle-level, and NLO+NNLL and LO+NNLL theory predictions [3].

3.2. Inclusive jet production at 8 and 13 TeV

The inclusive jet cross sections have been measured using the ATLAS 8 TeV dataset [4]. Jets are reconstructed with the anti-k_{T} algorithm with jet radius parameter values of $R = 0.4$ and $R = 0.6$, in the kinematic region of the jet transverse momentum from $p_{\mathrm{T}} > 70$ GeV and $|y^{\mathrm{jet}}| < 3$. The cross

sections are measured double-differentially in the jet transverse momentum and rapidity, as shown in Fig. 3 (left). A fair agreement has been found in the comparison between the measured cross sections and the fixed-order NLO QCD calculations for different PDF sets, corrected for non-perturbative and electroweak effects.

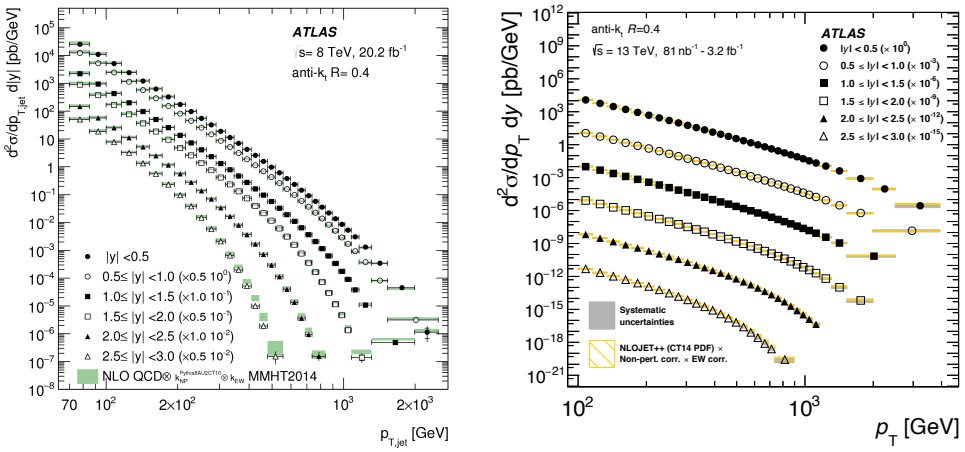


Fig. 3. Left (right): Inclusive jet cross section at 8 (13) TeV [4, 5] as a function of jet p_{T} in bins of jet rapidity. The data are compared to the NLO QCD prediction with the MMHT2014 PDF set. The error bars indicate the statistical uncertainty and the systematic uncertainty of the measurement added in quadrature.

The inclusive jet cross sections have also been measured at 13 TeV, using the 3.2 fb^{-1} ATLAS dataset [5]. The jets are reconstructed using the anti-k_{T} algorithm with radius parameter $R = 0.4$. The cross sections were measured following the same method of the 8 TeV analysis. The double-differentially cross sections for the 13 TeV measurement are shown in Fig. 3 (right). NLO and NNLO pQCD calculations, corrected for non-perturbative and electroweak effects, are compared to the measured cross sections. A good agreement has been found when considering the jet cross sections in individual jet rapidity bins independently. No significant deviations between measured cross sections and the fixed order NNLO QCD calculations are observed.

4. Exclusive production

In pp collisions, quasi-real photons can be emitted by both colliding protons, with a variety of final states produced. In these cases, the pp collisions can be then considered as a photon–photon ($\gamma\gamma$) scattering. Calculations of the cross section for the exclusive two-photon production are based on the

Equivalent Photon Approximation (EPA). These reactions can be studied at energies well beyond the electroweak energy scale at the LHC. The main backgrounds come from the single- and double-dissociative events, where one or both colliding protons fragment.

4.1. Exclusive di-lepton production at 7 TeV

The exclusive $\gamma\gamma$ production of lepton pairs, $\gamma\gamma \to \ell^+\ell^-$, has been measured using the 4.7 fb^{-1} ATLAS dataset at 7 TeV [6]. The exclusive selection is required demanding no tracks with $p_{\mathrm{T}} > 0.4$ GeV associated to the lepton vertex and, in addition, no tracks or vertices within at least 3 mm from the longitudinal isolation of the exclusive vertex. After requiring the dilepton mass to be outside a window of 70–105 GeV and restricting the lepton p_{T} to be below 1.5 GeV, the di-lepton acoplanarity distribution, $|1 - \Delta\phi_{\ell^+\ell^-}|/\pi$, is studied to discriminate the signal from the dissociative backgrounds. The measured fiducial cross sections for the exclusive di-electron and di-muon productions are shown in Fig. 4 (left). These results are in good agreement with the EPA predictions, corrected for absorptive corrections, and the CMS measurement [7].

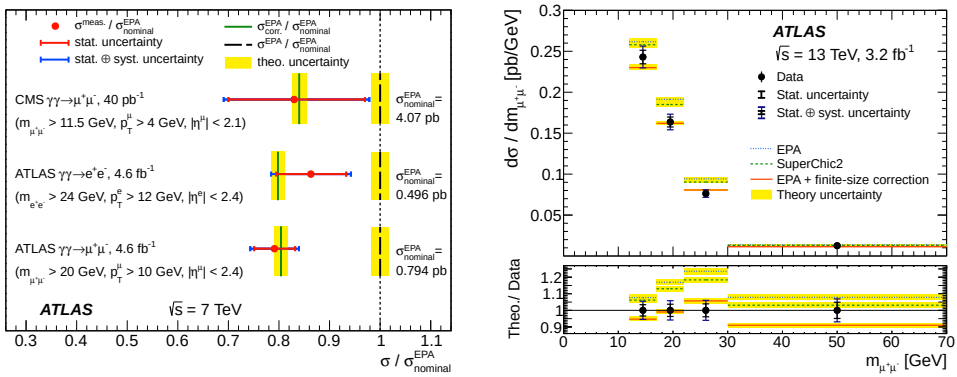


Fig. 4. (Colour on-line) Left: Comparison of the ratios of measured (points/red) and predicted (vertical solid/green lines) cross sections to the uncorrected EPA calculations (dashed/black line) [6]. Results for the muon and electron channels are also compared with a similar CMS measurement [7]. Right: Differential cross section in the muon pair mass for exclusive events, compared to the EPA and SuperChic2 models [8].

4.2. Exclusive di-muon production at 13 TeV

The exclusive $\gamma\gamma \to \mu^+\mu^-$ process has been studied using the 3.2 fb^{-1} ATLAS dataset at 13 TeV [8]. As in the previous section, a track veto and a longitudinal isolation cut are applied along with a requirement on

the di-muon transverse momentum, $p_{\mathrm{T}}^{\mu\mu} < 1.5$ GeV, in order to suppress dissociative events. The contribution from $Z \to \mu^+\mu^-$ events is avoided by selecting events in the di-muon mass window of 12–70 GeV. The acoplanarity of the muon pairs after these selections shows that the observed process can be well-modelled in terms of exclusive and single dissociative events, with a very small admixture of double dissociative events. Figure 4 (right) shows the measured differential cross section in the di-muon mass. The EPA model describes the data well, and better than the SuperChic2 model.

4.3. Exclusive W pairs production at 8 TeV

The exclusive W pairs production has been studied using the 20.3 fb^{-1} ATLAS dataset at 8 TeV [9]. This process can be exploited in estimating anomalous quartic gauge coupling (aQGC), $\gamma\gamma WW$, and study the exclusive Higgs production, in $e^{\pm}\nu\mu^{\mp}\nu$ final-state events. This analysis uses an exclusive selection similar to the one used in the previous sections, with a longitudinal isolation of 1 mm. The absence of the simulations of the dissociative backgrounds is taken into account multiplying the predicted $\gamma\gamma \to WW$ events by a factor 3.3, obtained by comparing the exclusive di-lepton yield in data with $m_{\ell\ell} > 160$ GeV to the Herwig++ prediction. Figure 5 (left) shows the distribution of $p_{\mathrm{T}}^{e\mu}$ in the signal region. The measured cross section for the exclusive W pair production is compatible to the Herwig++ predictions. The background-only hypothesis corresponds to a significance of 3σ. Limits on aQGC are obtained using event yields in the distribution of p_{T} of the electron–muon pair for $p_{\mathrm{T}}^{e\mu} > 120$ GeV and are compatible to those set by CMS [10], as shown in Fig. 5 (right).

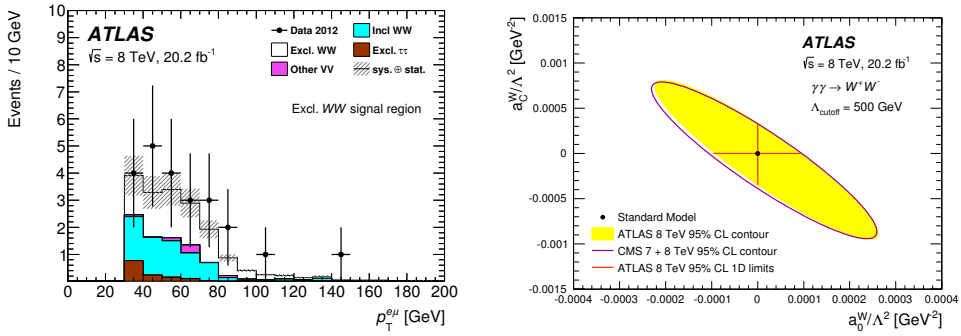


Fig. 5. Left: The $p_{\mathrm{T}}^{e\mu}$ distribution in the exclusive W^+W^- signal region. Right: The observed log-likelihood 95% confidence-level contour and 1D limits for the case with a dipole form factor with $\Lambda_{\mathrm{cutoff}} = 500$ GeV [9]. The CMS result [10] is shown for comparison.

5. Summary

This contribution summarizes the latest tests on QCD performed with the ATLAS detector, indicating the exceptionally wide range of physics that can be studied at the LHC. Very encouraging results, in agreement with the theoretical predictions, were found. The ATLAS Collaboration is looking forward to repeat and improve the measurements with the full Run-2 statistics.

REFERENCES

[1] ATLAS Collaboration, *JINST* **3**, S08003 (2008).
[2] ATLAS Collaboration, *Phys. Rev. D* **96**, 092008 (2017).
[3] ATLAS Collaboration, *Phys. Rev. Lett.* **121**, 092001 (2018) [arXiv:1711.08341 [hep-ex]].
[4] ATLAS Collaboration, *J. High Energy Phys.* **1709**, 20 (2017).
[5] ATLAS Collaboration, *J. High Energy Phys.* **1805**, 195 (2018) [arXiv:1711.02692 [hep-ex]].
[6] ATLAS Collaboration, *Phys. Lett. B* **749**, 242 (2015).
[7] CMS Collaboration, *J. High Energy Phys.* **1201**, 52 (2012).
[8] ATLAS Collaboration, *Phys. Lett. B* **777**, 303 (2018).
[9] ATLAS Collaboration, *Phys. Rev. D* **94**, 032011 (2016).
[10] CMS Collaboration, *J. High Energy Phys.* **1608**, 119 (2016).